Journal of Thermal Analysis and Calorimetry, Vol. 80 (2005) 579–583

THERMAL PROPERTIES OF THE MAGNETIC $RuSr_2GdCu_2O_8$ SUPERCONDUCTOR

G. A. Costa[1*], *A. Ubaldini*[1], *C. Artini*[1], *M. M. Carnasciali*[2] *and R. Masini*[3]

[1]INFM (LAMIA) and DCCI, Università di Genova, Via Dodecaneso 31, 16146 Genova, Italy
[2]INSTM and DCCI, Università di Genova, Via Dodecaneso 31, 16146 Genova, Italy
[3]CNR-IMEM, Sezione di Genova, Via Dodecaneso 33, 16146 Genova, Italy

A thermal study was performed on the $RuSr_2GdCu_2O_8$ (Ru-1212) magnetic superconductor phase to investigate the effect of the annealing treatments in flowing O_2 on the stability limit of the phase and on its structural, magnetic and transport properties.

DTA-TG measurements were utilized to determine the decomposition process and the dependence of the decomposition temperature on the annealing atmosphere.

The decomposition of the Ru-1212 phase was found sensitive to the oxygen partial pressure and increases with P_{O_2} and the annealing time.

The annealing treatments exert a depressing effect on the strength of the magnetic interaction, an enhancement on the superconductive properties and the vanishing of the magnetostriction.

A decomposition reaction of Ru-1212 phase was proposed and discussed.

Keywords: *DTA-TG, EGA, phase stability, ruthenates, superconductivity*

Introduction

$RuSr_2GdCu_2O_8$ is the most studied member of the ruthenocuprates, a class of superconducting materials that were synthesized for the first time in 1995 [1]. The compounds belonging to this class have very interesting features, as superconductivity and magnetism coexist [1, 2] and the temperature at which the magnetic ordering occurs, T_M, is higher than the superconducting transition, T_c. In particular, for $RuSr_2GdCu_2O_8$ T_M and T_c are about 132 and 50 K, respectively.

Ru-1212, has an oxygen-deficient triple perovskitic structure similar to that of $YBa_2Cu_3O_7$ (YBCO), where *Y* is formally replaced by Gd, Ba by Sr and Cu in the charge reservoir by Ru, so that the CuO chains are substituted by RuO_6 octahedra. Actually, the ground state is considered to be antiferromagnetic with a ferromagnetic component in the *ab* plane due to the lack of symmetry caused by the canting of the RuO_6 octahedra. Magnetism and superconductivity can coexist because they are supposed to act in different layers, namely the first one in the layer containing Ru, and the second one in the Cu layer.

Such coexistence implies, moreover, that both states develop in one thermodynamic phase, therefore a strict spatial chemical and structural uniformity of the samples is a key question for the study of such hybrid system. Homogeneity and phase purity of Ru-1212 samples were confirmed by X-ray and neutron diffraction studies even though a question of phase purity of Ru-1212 samples has been arisen recently. Attention was drawn to the fact that neither thermal neutrons nor X-ray diffraction experiments can detect substitutions between Ru and Cu without ambiguity due to the nearly same cross sections and ionic radii of these elements.

The wide spread of structural data reported in literature (a=3.82–3.84; c=11.48–11.59 Å) [2–13] (and the lack of suitable single crystal data) are indicative either of an extended solid solubility, or cationic disorder, or a possible incorrect attribution of the structure to the P4/mmm space group. Recently Martinelli *et al.* [14] and Cimberle *et al.* [15] have observed the development of an orthorhombic structure during the homogenization process.

An upper stability limit of the Ru-1212 phase at 1060°C has been moreover reported [9, 11], indicating that the phase starts to decompose at this temperature in oxygen which implies that the high temperature annealing usually performed in the synthesis may lead to a phase separation into FM and SC phases. Furthermore, Matveev *et al*. [9, 13, 16] recently reported that RuO_2 may be lost during the preparation or annealing at high temperatures above 900°C.

It is generally accepted that the annealing treatments have a homogenizing and an ordering effect and do not affect the total oxygen content [3], unlike for YBCO, where the oxygen content can be tuned with important consequences on its critical tempera-

---

[*] Author for correspondence: COSTA@chimica.unige.it

1388–6150/$20.00

Akadémiai Kiadó, Budapest, Hungary
Springer, Dordrecht, The Netherlands

ture [17]. As the thermal treatments in O_2 lead to an increase of the *c* cell parameter [18], and hence to higher distance between the Ru layers, the magnetic interaction should weaken as a consequence of the annealings. For this reason we expect a different temperature dependence of the cell parameters in the as-prepared and annealed samples: a magnetostriction effect should be visible in the cell parameters near T_M, as usually observed in ferromagnetic materials.

The aim of this work is to investigate the thermal stability of Ru-1212 powders by TG-DTA-EGA analysis and relate the observed temperature dependence of the cell parameters of as-prepared and long annealed samples as well as the effects of the long thermal treatment on their physical properties.

Experimental

Samples were prepared by a solid state reaction by mixing RuO_2, (Aldrich 3N) $SrCO_3$, (Aldrich 4N5) Gd_2O_3 (Aldrich 3N) and CuO (Aldrich 4N+) powders, as previously reported [18, 19]. The preparation requires many thermal treatments and annealings in different atmospheres. Sample A (as-prepared sample) underwent the thermal treatments in flowing O_2 as reported in [18, 19]; subsequent annealing of the as-prepared samples in flowing O_2 at 1060°C for one week and one month resulted in samples B and C, respectively.

All samples were characterized by the usual techniques in our laboratory. The purity of the samples was checked by room temperature X-ray diffraction using a Philips PW 1830 diffractometer, by micro-Raman spectroscopy using a Renishaw System 2000 Raman imaging microscope, by standard optical micrographic techniques, and SEM EDAX analysis. Density was determined by optical inspection and Bethlehem balance. The thermal behaviour of electrical resistivity was determined by the standard four-point technique using a 1 mA current. The temperature dependence of the cell parameters was determined by low temperature X-ray diffraction between 15 and 300 K in a Huber Guinier diffractometer. Thermal decomposition data (TG, DTA, EGA) in different atmospheres and partial pressures of O_2 were collected by means of a Netzsch STA 408 thermal analyser equipped with a Leybold evolved gas analyser (Inficon Quadrex 200).

Results and discussion

No traces of secondary phases were detected by room temperature X-ray and micro-Raman analyses for any of the samples. All peaks of the diffraction patterns can be indexed on the basis of the generally accepted tetragonal structure with the *P4/mmm* space group, yielding the cell parameter values reported in Table 1.

Table 1 Cell parameters of samples A, B and C

Sample	*a*/Å	*c*/Å
A	3.840(0)	11.560(1)
B	3.838(0)	11.579(1)
C	3.838(0)	11.576(1)

It is possible to observe that, while the *a*-axis is almost constant the *c*-axis first increases as a consequence of the annealing and then remains constant. In principle, this could be due to an increased oxygen content as well as to a structural ordering caused by the annealing process.

The DTA analyses performed in flowing O_2 on samples A, B and C are shown in Fig. 1 (TG data omitted for clarity). T_{onset} and T_{peak} are also indicated in Fig. 1. Even though the sample purity was crystallographically derived, it was further confirmed by the STA-TG-DTA data. No appreciable presence of a second early decomposing phase is in fact detectable in the curves, moreover the characteristic temperatures, T_{onset} and T_{peak}, both change regularly as a function of the annealing time at 1060°C (indicating a successful homogenization procedure and a safe annealing temperature). As expected, the more prolonged annealing the higher the onset of the decomposition temperature, indicating a more stable compound.

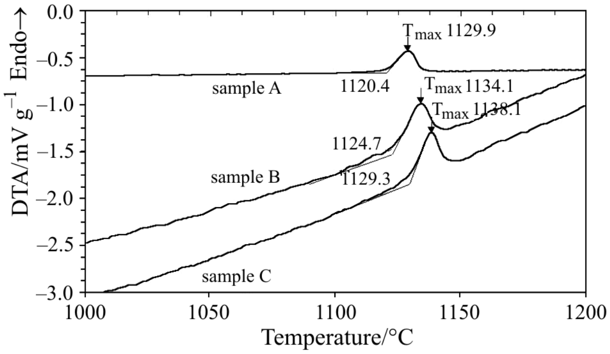

Fig. 1 DTA analysis of samples A, B and C in flowing O_2

In agreement, the TG data (omitted in the figure) show a similar temperature dependence, no presence of second early decomposing phases and the same (within the error limits) mass loss at the transition. TG and DTA data of sample B, obtained at different P_{O_2}, are reported in Fig. 2.

Notice that in P_{O_2}=1.01 bar (pure oxygen) the sample mass is almost constant until about 1120°C, where the sample mass begins to decrease. The mass loss is over at 1138°C and the total change is about 1.2% (about 1.4% in air P_{O_2} =0.2 bar). Correspondingly, a

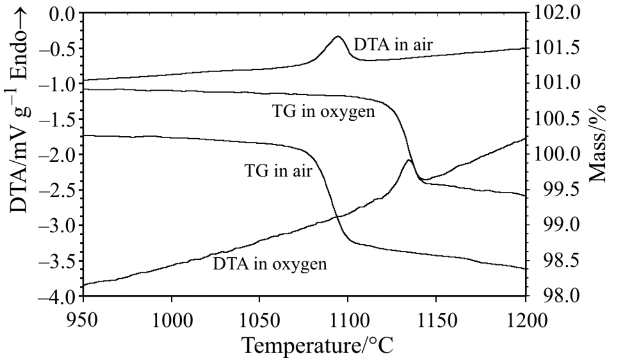

Fig. 2 DTA-TG analysis performed on sample B in air and flowing O_2 (TG corrected for instrumental drift)

major endothermic effect begins to show at 1120°C and its maximum is reached at 1134°C.

Thus, the most characterizing aspects of Figs 1 and 2 can be summarized as follows:

- $RuSr_2GdCu_2O_8$ samples are shown by different techniques to be pure
- the amount of phase decomposition is sensitive to the oxygen partial pressure
- the decomposition temperature increases with P_{O_2}
- the decomposition temperature increases with the annealing time of the samples

No special gas evolution, except the carrier gas, was observed by EGA during the thermal analysis.

According to Zhigadlo *et al.* [11], the Ru-1212 phase decomposition reaction in flowing O_2 involves $RuSr_2GdO_6$ and CuO:

$$RuSr_2GdCu_2O_8 \rightarrow RuSr_2GdO_6 + 2CuO \qquad (1)$$

Nevertheless, it is interesting to observe that a decomposition mechanism of $RuSr_2GdCu_2O_8$ simply leading to $RuSr_2GdO_6$ and CuO can not explain the observed mass loss, as O_2 is not released. Conversely it should be noticed that at the decomposition temperature of Ru-1212, cuprite (Cu_2O) is a stable copper oxide, too; for this reason it would be possible that the product of the decomposition is Cu_2O but the mass loss would then be practically twice (about 2.3%) than the one observed.

However, considering that the ruthenatic decomposition product does not affect significantly the activities in the Cu–O phase diagram [20–22], we note that at P_{O_2}=1 bar and at T~1130°C, CuO partly decomposes to a liquid L_2 whose X_O is 0.39 [22] at the eutectic Cu_2O–CuO.

In O_2, the mass loss in our sample (about 1.2%) corresponds to an O_2 mass loss of about 6% from the total amount of CuO or, in other words, to the decomposition of ~60% of the initial CuO; this evidence is in accordance with the phase diagram. Thus, our data indicate that it is reasonable that the decomposition proceeds following the reaction (1), but that contemporarily a part of CuO decomposes into L_2, releasing O_2, and giving rise to the following overall process:

$$\begin{aligned} RuSr_2GdCu_2O_8 \rightarrow RuSr_2GdO_6 + \\ +2(1-x)CuO + 2xL_2(CuO_z \text{ composition}) + \\ +x(1-z)O_2 \end{aligned} \qquad (2)$$

The fact that an appreciable mass loss is still detected even after the end of the decomposition reaction (the high temperature tail of the TG curve) can be explained by the increasing amount of CuO turned in L_2 increasing temperature as reported in the Cu–O phase diagram [22].

The temperature of the endothermic peak maximum shifts from 1140°C (P_{O_2}=1.01 bar) to 1090°C in air (P_{O_2}=0.2 bar) and to an even lower value (1060°C – data not shown) in argon. The greatest mass variation at the decomposition occurs in argon, viz. 1.67%. This is exactly what we expect from reaction (2), in the sense that decreasing the oxygen partial pressure decreases the stability of CuO.

The reaction mechanism proposed by [16] could be possible in non homogeneous Ru-1212 due to the loss of RuO_2. Stability of ruthenium oxides can be very low at moderate temperatures expecially for the phases with higher oxygen content, i.e. RuO_3 and RuO_4, or in humid or reducing environments [24–26]. Ruthenium depletion would lead to a higher phase inhomogeneity, lower crystallinity, lower decomposition temperature and then lower thermal stability. We may here confirm, by X-ray, TG-DTA, and micro-Raman analyses, that prolonged annealing at temperatures up to 1060°C in our samples resulted in a more stable product.

Thermal results suggest that the observed variation of the cell parameters can be ascribed to a structural reorganisation rather than changes in the oxygen content. It is quite reasonable to expect that the differences between the structures of annealed and unannealed samples would have some consequences on their physical properties.

In Figs 3a and b the cell parameters as a function of temperature are reported: in both cases the cell constants slightly decrease as the temperature is reduced. The *c* parameter of the as-prepared sample (A) displays a quite complex trend: it first decreases almost linearly starting from high temperature and in the proximity of T_M it shows a local minimum at about 125 K. Sample B, on the other hand, shows a different behaviour: *c* parameter behaves almost ideally with the temperature resembling most of the metals (linear decrease with temperature and flattening below LN_2 temperatures). No hint of magnetostriction is detected in agreement with the experimental data reported by Mc Laughlin *et al.* [23] in a similar sample. Any deviation from the ideal behaviour is not detected in the

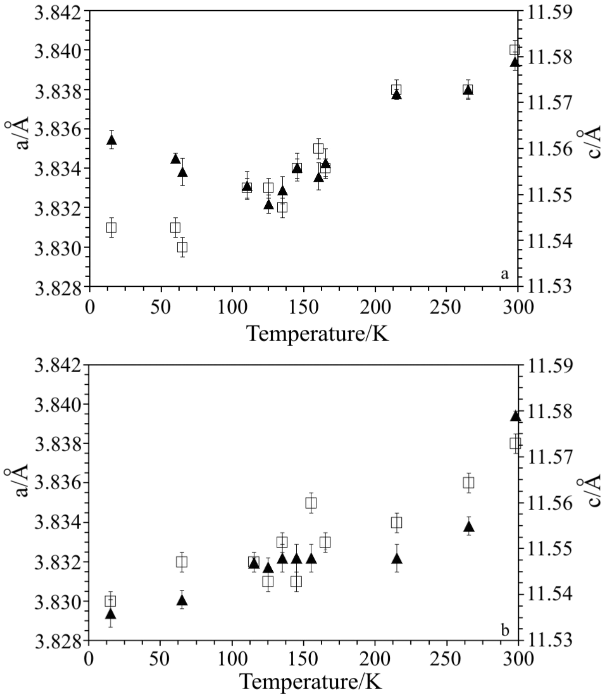

Fig. 3 Cell parameters of samples a – A and b – B as a function of temperature (lattice parameter *c* full triangles; lattice parameter *a* open squares)

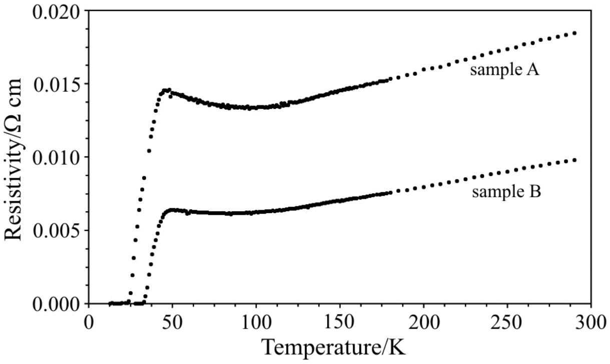

Fig. 4 Resistivity as a function of temperature

trend of the parameter *a* both in annealed and unannealed samples in accordance with the fact that there is no variation of this parameter upon annealing.

A similar trend in many respects can be found in the transport properties. In Fig. 4 we present the temperature dependencies of the measured resistivities: both samples exhibit a metal-like behaviour in the normal state and a small semiconducting upturn below 100 K with an onset to the superconducting state at about 45 K. Although the transitions of the two samples begin at the same temperature, it is worth noting that their width decreases with the annealing. A broad double-step structure is noticeable in the transition region for sample A (ΔT_c=23 K), while sample B displays a single sharp transition (ΔT_c=15 K). The measured resistivity value decreases with the annealing as does the magnitude of the upturn just before the superconducting transition, cf. Fig. 4.

It must be pointed out, however, that such variations in conductivity are not related to morphological effects: SEM analyses in fact show a very uniform structure for both A and B samples, grain growth is not observed at all [27] and density is only slightly enhanced.

The double transition has to do with the extrinsic character of a granular superconductor like HTSC sintered ceramic and is indicative of an intra- and an inter-granular coupling. The reported variations of the electrical properties in the superconducting transition region of both the samples confirm the improving and ordering effect of the annealing treatments performed. The two resistivity curves exhibit, moreover, different features even near T_M: a slight decrease (change of slope) in the resistivity curve is observed in sample A behaviour, while sample B resistivity follows a linear trend in this region. The evidence of an irregularity in the temperature dependence of resistivity near T_M is easily detectable in ferromagnetic materials. Hence, the observed behaviour in the cell parameters and in the resistivity curves near T_M can be related to the variations of the magnetic properties of the material due to annealing in O_2.

As described before, a consequence of the annealing treatment is the increase of the *c* parameter; this means that the mean distance between the Ru–O layers raises and that the magnetic coupling strength between Ru moments, belonging to different layers, weakens. We interpret the observed behaviour of the *c* parameter in sample A as an indication of magnetostriction that manifests itself in the *c* direction because it is a consequence of the magnetic coupling, taking place in this direction. Considering that the distance between the Ru–O layers increases upon annealing, the lack of visibility of the irregularity in the trend of the cell parameters of sample B can be explained in terms of weakened magnetic coupling. This conclusion is corroborated by the results of the resistivity measurements *vs.* *T*, performed on both samples. The decreased visibility of the kink in the resistivity behaviour of the B sample is a sign of the depressing effect that the annealing treatments exert on the magnetic properties of the material. As this trend matches with the described improvement of the superconductive properties, we are confirmed of the idea that in Ru-1212 magnetic and superconducting orders do not destroy each other but influence each other.

Conclusions

We studied the thermal properties of the magnetic superconductor Ru-1212 through low temperature X-ray diffraction and simultaneous DTA-TG measurements.

We observed the presence of a magnetostriction effect in the samples not submitted to a long annealing in flowing O_2; this effect is not visible in the annealed sample. From the results of the DTA-TG measurements it is possible to conclude that the effect of the annealing treatments is an increase in the total stability. We can also state that it influences by enhanced ordering in agreement with the orthorhombic distorsion earlier observed [14].

We conclude that the smoothing of the irregularity at the magnetic transition in the temperature dependence of the thermal expansion and in the electrical resistivity in annealed samples is related to the weakening of the magnetic coupling between the Ru–O layers along the *c* direction.

References

1 L. Bauernfeind, W. Widder and H. F. Braun, Phys. C, 254 (1995) 151.
2 V. P. S. Awana, M. Karppinen and H. Yamauchi, Studies of High Temperature Superconductors, International Book Series, Vol. 46, A. Narlikar (Ed.), Nova Science Publisher, New York 2003, p. 77.
3 M. Matvejeff, V. P. S. Awana, L.-Y. Jang, R. S. Liu, H. Yamauchi and M. Karppinen, Phys. C, 392–396 (2003) 87.
4 D. Z. Wang, H. I. Ha, J. I. Oh, J. Moser, J. G. Wen, M. J. Naughton and Z. F. Ren, Phys. C, 384 (2003) 137.
5 V. P. S. Awana, S. Ichihara, M. Karppinen and H. Yamauchi., Phys. C, 378–381 (2002) 249.
6 T. P. Papageorgiou, T. Herrmannsdörfer, R. Dinnebier, T. Mai, T. Ernst, M. Wunschel and H. F. Braun, Phys. C, 377 (2002) 383.
7 R. Ruiz-Bustos, J. M. Gallardo-Amores, R. Sáez-Puche, E. Morán and M. A. Alario-Franco, Phys. C, 382 (2002) 395.
8 G. M. Kuz'micheva, V. V. Luparev, E. P. Khlybov, I. E. Kostyleva, A. S. Andreenko and K. N. Gavrilov, Phys. C, 350 (2001) 105.
9 A. T. Matveev, A. Kulakov, A. Maljiuk, C. T. Lin and H. U. Habermeier., Phys. C, 400 (2003) 53.
10 I. Felner, U. Asaf, S. Reich and Y. Tsabba, Phys. C, 311 (1999) 163.
11 N. D. Zhigadlo, P. Odier, J. Ch. Marty, P. Bordet and A. Sulpice, Phys. C, 387 (2003) 347.
12 D. P. Hai, S. Kamisawa, I. Kakeya, M. Furuyama, T. Mochiku and K. Kadowaki, Phys. C, 357–360 (2001) 406.
13 A. T. Matveev, E. Sader, V. Duppel, A. Kulakov, A. Maljiuk, C. T. Lin and H. U. Habermeier, Phys. C, 403 (2004) 231.
14 A. Martinelli, C. Artini, R. Cimberle, G. A. Costa, M. Ferretti, R. Masini and P. Mele, Phys. Rev. B, 69 (2004) 052507/1.
15 M. R. Cimberle, R. Masini, E. Gilioli, C. Artini, G. A. Costa, M. Ferretti, P. Mele and A. Martinelli, Phys. C, 408–410 (2004) 187.
16 A. T. Matveev, A. N. Maljuk, A. Kulakov, C. T. Lin and H. U. Habermeier, Phys. C, 407 (2004) 139.
17 R. J. Cava, B. Batlogg, C. H. Chen, E. A. Rietman, S. M. Zahurak and D. Werder, Nature, 329 (1987) 423.
18 C. Artini, M. Carnasciali, G. A. Costa, M. Ferretti, M. R. Cimberle, M. Putti and R. Masini, Phys. C, 377 (2002) 431.
19 R. Masini, C. Artini, M. R. Cimberle, G. A. Costa, M. Carnasciali and M. Ferretti, Ruthenate and rutheno-cuprate materials, Lecture Notes in Physics Series, Vol. 603, C. Noce, A. Vecchione, M. Cuoco and A. Romano (Eds) Springer Verlag, Berlin 2002, p. 222.
20 A. B. Bykov, L. N. Demianets, I. P. Zibrov, G. V. Kanunnikov, O. K. Melnokov and S. M. Stishov, J. Cryst. Growth, 91 (1988) 302.
21 J. P. Neumann, T. Zhong and Y. A. Chang, Bull. Alloy. Phase Diagr., 5 (1984) 136.
22 B. Hallstedt, D. Risold and L. J. Gauckler, J. Phase Equilib., 15 (1994) 483.
23 A. C. Mc Laughlin, J. P. Attfield and J. L. Tallon, Int. J. Inorg. Mat., 2 (2000) 95.
24 C. A. Georg, P.Triggs and F. Levy, Mater. Res. Bull., 17 (1982) 105.
25 M. Prudenziati, B. Morten and E. Travan, Mater. Sci. Eng. B, 98 (2003) 167.
26 B. Brunetti, P. Scardala and V. Piacente, Mater. Chem. Physics, 84 (2004) 145.
27 C. Artini, M. Carnasciali, G. A. Costa, M. Ferretti and R. Masini, Advances in science and technology, P. Vincenzini and S. Ceresara (Eds), Tecna, Faenza 2003, p. 77.